Chemistry–A European Journal
Research Article
doi.org/10.1002/chem.202301418
Chemistry Europe
European Chemical Societies Publishing
www.chemeurj.org

Special Collection

Synthesis, Structural Characterization, and Bonding of Molecular Heavier Beryllium Chalcogenides

Corinna Czernetzki,[a, b] Tobias Tröster,[a, b] Lukas Endres,[a, b] Franziska Endres,[a, b] Merle Arrowsmith,[a, b] Annalena Gärtner,[a, b] Felipe Fantuzzi,[c] and Holger Braunschweig*[a, b]

Abstract: The reactions of a cyclic alkyl(amino)carbene (CAAC)-stabilized beryllium radical with E_2Ph_2 (E = S, Se, Te) and of a beryllole with HEPh (E = S, Se) yield the corresponding beryllium phenylchalcogenides, including the first structurally authenticated beryllium selenide and telluride complexes. Calculations show that their Be–E bonds are best described by the interaction between the Be^+ and E^- fragments, with Coulombic forces accounting for ca. 55% of the attraction and orbital interactions dominated by the σ component.

Introduction

Due to its high toxicity,[1–3] the coordination chemistry of beryllium lags significantly behind that of the heavier alkaline earth metals[4–9] and has been carried out mainly in silico since the 1990s.[10] The increasing interest in low-valent main group chemistry in recent years, however, has also led to a renaissance in experimental beryllium chemistry,[11–16] culminating in the isolation of the first Be(0)[17] and Be(I)[18,19] complexes (e.g. **I** and **II**, Figure 1). These owe their stability to the strong σ-donor and π-acceptor properties of the cyclic alkyl(amino)carbene (CAAC) ligand(s), which has been raising vehement discussion about the validity of their metal oxidation state.[20–22] More recently, our group also reported the first antiaromatic beryllacycle, compound **III**, which is isoelectronic to the cyclopentadiene cation and can be reduced to an aromatic berrylole dianion.[23]

Beryllium chalcogenide materials present high hardness, resistivity, thermal conductivity and radiation stability, which make BeO ceramics a material of choice in nuclear reactors.[24] Heavier beryllium chalcogenides also find uses as dopants in alloys for optoelectronic applications, albeit with limitations due to their toxicity.[25,26] In contrast, molecular beryllium chalcogenide complexes have been less widely explored. While the high oxophilicity of beryllium makes beryllium alkoxides particularly easy synthetic targets,[11–15] examples of heavier beryllium chalcogenide complexes remain scarce. Diorgano- and diaminoberyllium complexes are known to undergo hydrolysis reactions with thiols and selenols to form beryllium dichalcogenides (Figure 1a).[27–32] Furthermore, beryllium alkoxides and halides undergo salt elimination reaction with lithium sulfides to yield the corresponding beryllium sulfides (Figure 1b).[33–35] Finally, CS_2 was shown to insert into Be–N bonds to yield the corresponding dithiocarbamates (Figure 1c).[36] Overall, only three organosulfide beryllium complexes have been structurally authenticated,[24,33,34] and no examples of heavier organoselenide or -telluride complexes are known to date.

In this contribution we report the synthesis of heavier tricoordinate beryllium phenylchalcogenides by reaction of

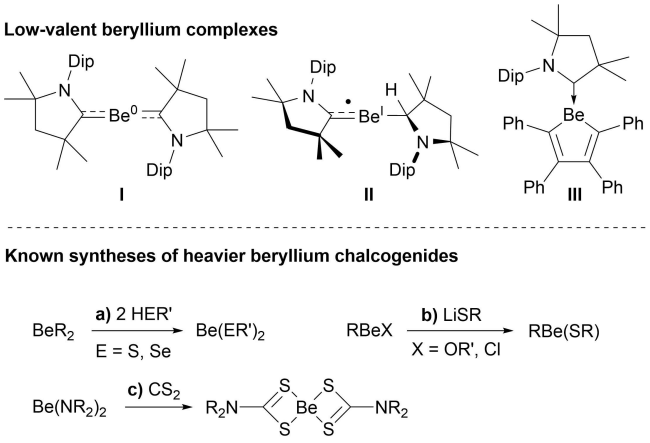

Figure 1. Examples of recent low-valent beryllium complexes and literature-known synthetic routes to heavier beryllium organochalcogenides. Dip = 2,6-$iPr_2C_6H_3$.

[a] C. Czernetzki, Dr. T. Tröster, L. Endres, F. Endres, Dr. M. Arrowsmith, Dr. A. Gärtner, Prof. Dr. H. Braunschweig
Institute for Inorganic Chemistry
Julius-Maximilians-Universität Würzburg
Am Hubland, 97074 Würzburg (Germany)
E-mail: h.braunschweig@uni-wuerzburg.de

[b] C. Czernetzki, Dr. T. Tröster, L. Endres, F. Endres, Dr. M. Arrowsmith, Dr. A. Gärtner, Prof. Dr. H. Braunschweig
Institute for Sustainable Chemistry & Catalysis with Boron
Julius-Maximilians-Universität Würzburg
Am Hubland, 97074 Würzburg (Germany)

[c] Dr. F. Fantuzzi
School of Chemistry and Forensic Science
University of Kent
Canterbury, Park Wood Rd, CT2 7NH (UK)

Supporting information for this article is available on the WWW under https://doi.org/10.1002/chem.202301418

Special Collection Part of a Special Collection on the p-block elements.

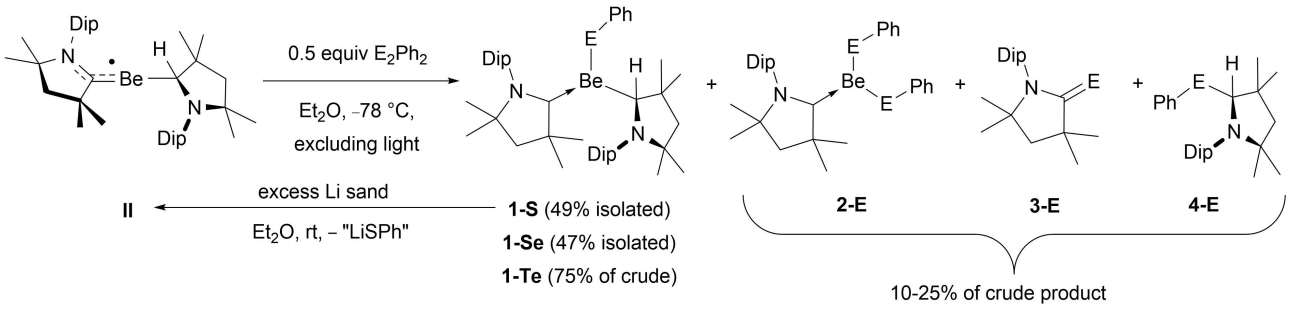

Scheme 1. Reactivity of beryllium radical **1** with dichalcogenides. Isolated yields in parentheses.

E_2Ph_2 (E = S, Se, Te) with the beryllium radical **II**, and by chalcogenolysis of an endocyclic Be–C bond of beryllole **III** with HEPh (E = S, Se), providing the first solid-state structures of molecular beryllium selenides and a telluride.

Results and Discussion

The addition of the diphenyldichalcogenides E_2Ph_2 (E = S, Se, Te) to the beryllium radical **II** in toluene at −78 °C with subsequent slow warming to room temperature yielded complex mixtures of products. For E = S, Te, the main reaction product was the racemic beryllium chalcogenide complex **1-E**. For E = Te the main side-product was the CAAC-chalcogen adduct **3-Te**.[37] For E = S the main side-product was **4-S**, which was confirmed in an independent synthesis by treating CAAC with PhSH. Furthermore, a few crystals of the beryllium dichalcogenide **2-S**, which results from the displacement of the CAACH ligand of **1-S** by a phenylsulfide substituent, were isolated and characterized by X-ray structural analysis (see Figure S29 in the Supporting Information). For E = Se, the only identifiable reaction by-products were **3-Se** and **4-Se**. The selectivity of the reactions was drastically improved (10–15% side-products in the crude) by carrying them out in the dark and changing the solvent to diethyl ether, which enabled the isolation of **1-S**, **1-Se** and **1-Te** as orange crystalline solids in moderate to good yields (47–75%, Scheme 1).[38] It is noteworthy that the reduction of **1-S** with lithium sand in diethyl ether regenerated the beryllium radical **II**. The formation of the beryllium chalcogenide species **1-E** and **2-E** from the reaction of **II** with E_2Ph_2, which is known to react by homolytic E–E bond cleavage, is indicative of a beryllium-centered radical in **II**, thus providing clear experimental evidence for the assignment of the +1 oxidation state to the beryllium center in this species.

The ^{9}Be NMR spectra of **1-E** show broad resonances (full width at mid-height: fwmh ≈ 420–550 Hz) at 20, 22 and 24 ppm, for E = S, Se and Te, respectively, the downfield shift down the group reflecting the diminishing p-orbital overlap. Power's tricoordinate beryllium organosulfide $(Et_2O)Be(Tp^*)(SMes^*)$ (Tp^* = 2,6-(2,4,6-$Me_3C_6H_2$)$_2C_6H_3$, Mes^* = 2,4,6-tBu$_3C_6H_2$) shows a ^{9}Be NMR resonance at 17.4 ppm (fwmh ≈ 540 Hz), slightly upfield of **1-S**.[33] The ^{77}Se NMR spectrum of **1-Se** and the ^{125}Te NMR spectrum of **1-Te** show a singlet at 205.0 and 157 ppm, respectively. The ^{1}H NMR spectra show the characteristic resonance pattern of CAAC- and CAACH-stabilized beryllium complexes,[19] with the Be*CH* singlet at ca. 3.2 ppm and two sets of unsymmetrical *i*Pr-CH resonances at ca. 4.6 and 3.7 ppm (two sharp septets) for the CAAC ligand and 3.4 and 2.5 ppm (two broad septets) for the CAACH ligand. The UV-vis spectra of **1-E** showed a very broad, low-intensity absorption band, starting around 380 nm and trailing up to 600 nm, with a maximum at 449, 459 and 417 nm for E = S, Se and Te, respectively.

Orange single crystals of **1-S**, **1-Se** and **1-Te** provided X-ray crystallographic data for their solid-state structures (Figure 2 and Figure S29 in the Supporting Information; Table 1). In all three compounds the Be plane is near-orthogonal to the plane of the CAAC ligand (torsion angle |N1–C1–Be1–E| 80.2(2)–95.4(3)°). In **1-S**, the EPh moiety is oriented so that the phenyl

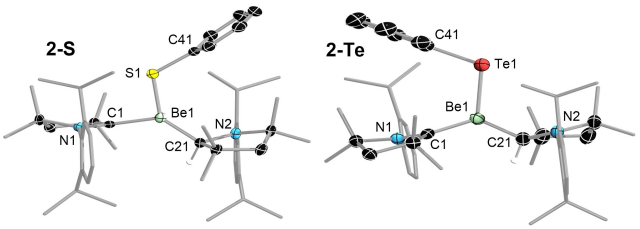

Figure 2. Solid-state structures of **1-S** and **1-Te**. Thermal displacement ellipsoids at 50%. Ellipsoids of ligand periphery and hydrogen atoms omitted for clarity, except for CAACH hydrogen atom at C21.

Table 1. ^{9}Be NMR shifts (ppm) and selected bond lengths (Å) and angles (°) for **1-E**.

	1-S	1-Se	1-Te
$\delta_{^9Be}$	20	22	24
Be1–E	2.0228(19)	2.179(3)	2.403(5)
Be1–C1	1.821(2)	1.797(4)	1.800(6)
Be1–C21	1.769(2)	1.790(4)	1.780(6)
C1–N1	1.311(3)	1.311(3)	1.304(5)
C21–N2	1.517(3)	1.517(3)	1.516(5)
C1–Be1–E	94.11(9)	116.72(17)	114.2(3)
C21–Be1–E	136.67(12)	116.32(17)	117.8(3)
Σ(∠Be1)	359.9(1)	359.4(2)	359.7(3)
Σ(∠C1)	359.3(1)	359.9(2)	359.9(3)
Be1–E–C41	119.08(7)	117.33(11)	112.81(16)
N1–C1–Be1–E	−80.2(2)	95.4(3)	91.7(4)
C1–Be1–E–C41	−172.92(8)	6.0(2)	6.0(4)

ring is positioned above the CAACH ligand (torsion angle C1–Be1–S1–C41 −172.92(8)°), whereas in **1-Se** and **1-Te**, the phenyl ring is rotated in the opposite direction, above the neutral CAAC ligand (C1–Be1–S1–C41 ca. 6°). Furthermore, whereas the EPh ligand is positioned symmetrically between the CAAC and CAACH ligands in **1-Se** and **1-Te** (C1–Be1–E ≈ C21–Be1–E ca. 116°), the SPh ligand in **1-S** is tilted towards to CAAC ligand, forming nearly a right angle (C1–Be1–E 94.11(9)°). The C1···S1 distance is reduced to 2.81 Å, enabling perhaps some orbital overlap between the lone pair at sulfur and the formally empty p orbital at C1. The Be–E distance increases down the group from 2.0228(19) Å in **1-S** to 2.403(5) Å in **1-Te**, in accordance with the increase in atomic radii. The Be–S bond length in **1-S** is longer than that in the only other structurally characterized tricoordinate beryllium organosulphides, (THF)Be(SMes*)$_2$ (1.991(7), 1.987(8) Å)[34] and (Et$_2$O)Be(Tp*)(SMes*) (1.984(3) Å),[33] presumably due to the stronger electron-donating ability of the CAAC ligand versus THF and Et$_2$O. As for **1-Se** and **1-Te**, they are the first examples of a beryllium selenide and telluride to be structurally authenticated.

The reaction of beryllole **III** with phenylthiol and -selenol in benzene at room temperature resulted in an instant color change from bright yellow to colorless, accompanied by an upfield shift of the ^{9}Be NMR resonance from 22.9 ppm to 18.0 (**5-S**, fwmh ≈ 580 Hz) and 20.6 (**5-Se**, fwmh ≈ 820 Hz) ppm, respectively (Scheme 2). The ^{1}H NMR spectra showed four magnetically inequivalent phenyl residues and a broad vinyl singlet at 7.73 and 7.99 ppm, respectively, indicative of ring-opening of an endocyclic Be–C bond and protonation of the resulting 1,2,3,4-tetraphenylbuta-1,3-dien-1-yl fragment. Furthermore, the ^{77}Se NMR spectrum of **5-Se** showed a singlet at 142 ppm. The upfield shifts in the ^{9}Be and ^{77}Se NMR spectra compared to **1-S** and **1-Se** reflect the more electron-donating character of the butadienyl ligand compared to CAACH. Compound **III** thus undergoes Be–C bond-cleaving hydrolysis

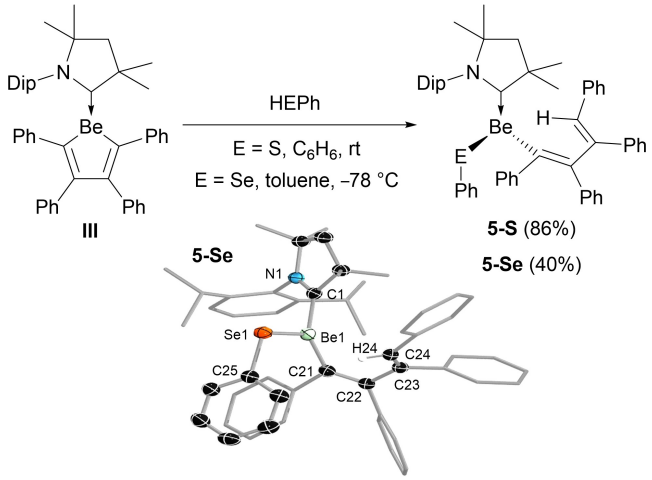

Scheme 2. Reactions of HSPh and HSePh with beryllole **III**. Isolated yields in parentheses. Solid-state structures of **5-Se**. Thermal displacement ellipsoids at 50 %. Ellipsoids of ligand periphery and hydrogen atoms omitted for clarity, except for vinyl proton at C24.

with HSPh and HSePh like other diorganoberyllium complexes.[30–32]

The structures of complexes **5-S** and **5-Se** were confirmed by X-ray crystallographic analyses (Scheme 2 and Figure S32 in the Supporting Information). The complexes show similar Be–S (2.034(4) Å) and Be–Se (2.168(3) Å) bond lengths to **1-S** and **1-Se**, respectively. The buta-1,3-dien-1-yl fragment shows distinct C–C double and single bond alternation (C21–C22, C22–C23, C23–C24: **5-S** 1.357(4), 1.492(4), 1.350(4) Å; **5-Se** 1.368(3), 1.491(3), 1.349(3) Å). The Be–C bond to the anionic butadienyl ligand (**5-S** 1.756(4) Å; **5-Se** 1.753(4) Å) is significantly shorter than to the CAAC donor ligand (**1-S** 1.827(4) Å; **1-Se** 1.813(4) Å) and slightly shorter than in precursor **III** (avg. 1.77 Å).

With the Be–Se (2.179(3) Å) and Be–Te (2.403(5) Å) bonds in **1-Se** and **1-Te**, respectively, being slightly longer than the sum of the corresponding covalent radii (r(Be) + r(Se) = 2.16 Å; r(Be) + r(Te) = 2.34 Å),[39] DFT calculations were undertaken to assess the bonding in complexes **1-E**. Structure optimizations at the ωB97X-D[40]/Def2-TZVP[41] level of theory provide good agreement with the X-ray structural data, and large singlet-triplet energy gaps have been found (see details of the computations in the Supporting Information). The computed Wiberg bond indices (WBIs)[42] of 1.19–1.22 and Mayer bond orders (MBOs)[43] of 0.83–0.89 for the Be–E bonds in **1-E** (E = S, Se, Te) are both indicative of single bonds (see Table S2 in the Supporting Information). Further investigation of the Be–E bonds in their corresponding equilibrium geometries was performed by energy decomposition analysis with natural orbitals for chemical valence model (EDA-NOCV)[44] calculations at the PBE0[45,46]-D3[47]/TZ2P level of theory. Two possible bonding situations, resulting from two distinct fragment pairs, were considered: a) an electron-sharing Be–E bond obtained by the combination of neutral radical [(CAAC)(CAACH)Be]$^\bullet$ and [EPh]$^\bullet$ fragments, and b) a dative $E^- \rightarrow Be^+$ interaction with the charged fragments $[EPh]^-$ and $[(CAAC)(CAACH)Be]^+$ to account for the formation of a polar bond.[48] The calculated orbital interaction energy ΔE_{orb} in the latter case (−81 to −84 kcal mol^{-1}) is less negative than in the former (−110 to −146 kcal mol^{-1}), revealing that the Be–E bonds in **1-E** are better described using the charged fragments (see Table S4 in the Supporting Information).[49] In all cases, electrostatic effects (ΔV_{elstat}) account for approximately 55 % of the attractive interaction terms and orbital interactions contribute to ca. 36 %. The breakdown of ΔE_{orb} into pairwise interactions indicates that the $E^- \rightarrow Be^+$ σ contribution is the dominant factor, but that a stabilizing $E^- \rightarrow Be^+$ π donation is also present. As shown in Figure 3, the main orbital interactions involved in $Te^- \rightarrow Be^+$ bonding in **1-Te** are primarily from $\Delta E_{orb\text{-}1}$ (55.6 %), representing the polarized Te–Be σ bond, and $\Delta E_{orb\text{-}2}$ (23.5 %), which corresponds to π donation from tellurium to the empty p_z orbital at beryllium. While a similar bonding picture is observed for **1-S** and **1-Se**, the total interaction energy decreases down group 16.

Finally, we calculated the thermodynamics of the formation of two molecules of **1-E** from **II** and E_2Ph_2 (see Supporting Information for details). The Gibbs free energy for the first step of the reaction, in which the E–E bond in E_2Ph_2 is broken and the first **1-E** molecule is formed, is close to zero for E = Se, Te

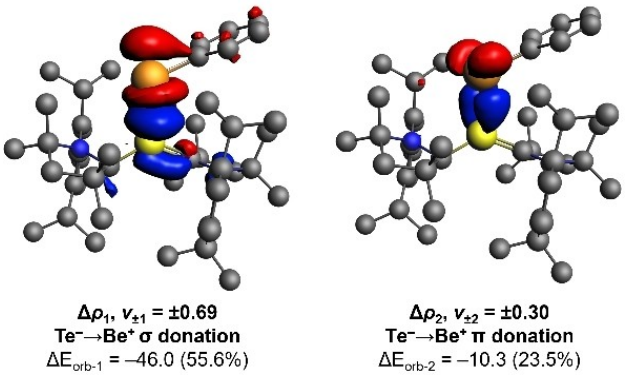

Figure 3. Plots of the deformation densities $\Delta\rho_1$ ($Te^- \rightarrow Be^+$ σ donation) and $\Delta\rho_2$ ($Te^- \rightarrow Be^+$ π donation) and the corresponding energies $\Delta E_{orb\text{-}1}$ and $\Delta E_{orb\text{-}2}$ (kcal mol^{-1}) of the main pairwise contributions associated with the orbital interaction term ΔE_{orb} in **1-Te** at the PBE0-D3/TZ2P level of theory. Values in parentheses are the percentage of the k^{th} pairwise orbital interaction $\Delta E_{orb\text{-}k}$ with respect to ΔE_{orb}. The eigenvalues $\nu_{\pm k}$ correspond to a charge transfer from orbital Ψ_{-k} to Ψ_{+k} in the NOCV representation. Isovalues: 0.003. Electron density flows from red to blue. Hydrogen atoms are omitted for clarity.

($\Delta G_1 = 0.5$–0.7 kcal mol^{-1}), and slightly negative for E = S ($\Delta G_1 = -7.7$ kcal mol^{-1}). While this step provides no accountable driving force for the reaction, for the second step of the reaction, in which the remaining radicals **II** and [EPh]$^\bullet$ combine to form a second **1-E** molecule, a substantial driving force of $\Delta G_2 = -30$ to -47 kcal mol^{-1} is observed. As expected, the reaction free energy is less negative as we move down the group, in line with weaker Be–E bonding.

Conclusions

To conclude, we have reported the synthesis of beryllium phenylchalcogenides via a) the radical reaction of a dicoordinate CAAC-stabilized beryllium radical with E_2Ph_2 (E = S, Se, Te) and b) the ring-opening hydrolysis of a tricoordinate beryllole with HEPh (E = S, Se). Reaction a) provides clear experimental evidence for the beryllium- rather than CAAC-centered radical nature of the disputed Be(I) precursor.[20–22] X-ray crystallographic analyses enabled the first structural authentication of Be–Se and Be–Te bonds, which DFT calculations show to be highly polarized single bonds, the Be–E interaction energy decreasing down group 16.

Experimental Section

NMR spectra, UV-vis spectra and details of the computations are provided in the Supporting Information.

Methods and Materials: All manipulations were performed either under an atmosphere of dry argon or *in vacuo* using standard Schlenk line or glovebox techniques. Deuterated solvents were dried over molecular sieves and degassed by three freeze-pump-thaw cycles prior to use. All other solvents were distilled and degassed from appropriate drying agents. Both deuterated and non-deuterated solvents were stored under argon over activated 4 Å molecular sieves. NMR spectra were acquired either on a Bruker Avance 500 (operating at 500 MHz for ^{1}H, 125 MHz for ^{13}C and 95 MHz for ^{77}Se) or a Bruker Avance 400 (operating at 400 MHz for ^{1}H, 56 MHz for ^{9}Be and 100 MHz for ^{13}C) NMR spectrometer. Chemical shifts (δ) are provided in ppm and internally referenced to the carbon nuclei ($^{13}C\{^1H\}$) or residual protons (^{1}H) of the solvent. Solid-state IR spectra were recorded on a Bruker FTIR spectrometer ALPHA II inside a glovebox. UV-vis spectra were acquired on a METTLER TOLEDO UV-vis-Excellence UV5 spectrophotometer inside a glovebox. Microanalyses (C, H, N, S) were performed on an Elementar vario MICRO cube elemental analyzer. Note: both elemental analyses and HRMS were carried out for all new compounds but in some cases these decomposed too rapidly and only one type of analysis was possible.

Be metal, S_2Ph_2, Se_2Ph_2, Te_2Ph_2, PhSH and PhSeH were purchased from various chemicals companies, transferred into a glovebox and used as received. CAAC (1-(2,6-diisopropylphenyl)-3,3,5,5-tetramethylpyrrolidin-2-ylidene),[50] [(CAAC)(CAACH)Be]$^\bullet$ (**II**, CAACH = 1-(2,6-di*iso*propylphenyl)-3,3,5,5-tetramethylpyrrolidin-2-yl)[19] and [(CAAC)Be(C_4Ph_4)] (**III**)[23] were synthesized following literature procedures.

Synthetic procedures

Synthesis of (CAAC)(CAACH)BeSPh, 1-S: A solution of freshly prepared **II** (131 mg, 0.223 mmol, 1.00 equiv.) in 5 mL of Et_2O was cooled to −78 °C and a solution of S_2Ph_2 (24.6 mg, 0.113 mmol, 0.500 equiv.) in Et_2O was added dropwise. The mixture was allowed to warm to room temperature and stirred for 1 h until its color changed from brown to red. Removal of all volatiles *in vacuo* provided an orange solid, which was washed with pentane until the washing phases became colorless, and then extracted with benzene. After removal of volatiles **1-S** was isolated as an orange solid (77.3 mg, 112 mmol, 49%). NMR data indicated contamination with small amounts of **4-S** (see independent synthesis of **4-S** below). ^{1}H NMR (500.1 MHz, C_6D_6): $\delta = 7.90$ (m, 2H, *o*-C*H*$_{Ph}$), 7.33 (dd, $^3J = 7.5$ Hz, $^4J = 1.9$ Hz, 1H, *m*-C*H*$_{Dip}$), 7.22 (t, $^3J = 7.5$ Hz, 1H, *p*-C*H*$_{Dip}$), 7.18 (m partly overlapping with solvent signal, 1H, C*H*$_{Ar}$), 7.09 (m, 2H, C*H*$_{Ar}$), 7.01 (m, 2H, C*H*$_{Ar}$), 6.95 (m 1H, C*H*$_{Ar}$), 6.84 (m 1H, C*H*$_{Ar}$), 4.58 (sept, $^3J = 6.7$ Hz, 1H, C*H*(CH$_3$)$_2$), 3.66 (sept, $^3J = 6.7$ Hz, 1H, C*H*(CH$_3$)$_2$), 3.44 (br. sept, 1H, C*H*(CH$_3$)$_2$), 3.17 (s, 1H, BeC*H*), 2.47 (br. sept, 1H, C*H*(CH$_3$)$_2$), 2.00 (d, $^2J = 12.0$ Hz, 1H, C*H*$_2$), 1.96 (d, $^2J = 12.0$ Hz, 1H, C*H*$_2$), 1.71 (br. d, 3H, CH(C*H*$_3$)$_2$), 1.62 (s, 3H, C(C*H*$_3$)$_2$), 1.55 (br. d, 3H, CH(C*H*$_3$)$_2$), 1.43 (d, $^3J = 6.7$ Hz, 3H, CH(C*H*$_3$)$_2$), 1.36 (d, $^3J = 6.7$ Hz, 3H, CH(C*H*$_3$)$_2$), 1.35 (d, $^3J = 6.7$ Hz, 3H, CH(C*H*$_3$)$_2$), 1.34 (d, $^3J = 6.5$ Hz, 3H, CH(C*H*$_3$)$_2$), 1.24 (s, 3H, C(C*H*$_3$)$_2$), 1.25 (d, 1H, C*H*$_2$, detected by HSQC), 1.22 (d, 1H, C*H*$_2$, detected by HSQC), 1.18 (s, 3H, C(C*H*$_3$)$_2$), 1.13 (three overlapping s, 9H, C(C*H*$_3$)$_2$), 0.99 (d, $^3J = 6.7$ Hz, 3H, CH(C*H*$_3$)$_2$), 0.97 (d, $^3J = 6.7$ Hz, 3H, CH(C*H*$_3$)$_2$), 0.76 (two overlapping s, 6H, C(C*H*$_3$)$_2$) ppm. $^{13}C\{^1H\}$ NMR (125.8 MHz, C_6D_6): $\delta = 254.7$ (C$_{carbene}$), 153.1 (*o*-C$_{Ar}$), 151.3 (*o*-C$_{Ar}$), 147.0 (NC$_{Ar}$), 146.1 (*o*-C$_{Ar}$), 146.0 (*o*-C$_{Ar}$), 143.4 (SC$_{Ar}$), 136.1 (NC$_{Ar}$), 134.7 (C*H*$_{Ar}$), 134.4 (*o*-C*H*$_{Ph}$), 129.9 (C*H*$_{Ph}$), 127.7 (C*H*$_{Ph}$), 126.3 (C*H*$_{Ar}$), 125.3 (C*H*$_{Ar}$), 125.0 (C*H*$_{Ar}$), 124.6 (C*H*$_{Ar}$), 124.4 (*m*-C*H*$_{Ar}$), 123.8 (C*H*$_{Ar}$), 81.4 (NC(CH$_3$)$_2$), 72.3 (BeCHN), 64.2 (NC(CH$_3$)$_2$), 60.5 (CH$_2$), 56.3 (C(CH$_3$)$_2$), 51.6 (CH$_2$), 41.3 (C(CH$_3$)$_2$), 34.7 (C(CH$_3$)$_2$), 34.3 (C(CH$_3$)$_2$), 32.7 (C(CH$_3$)$_2$), 31.5 (C(CH$_3$)$_2$), 31.1 (C(CH$_3$)$_2$), 30.3 (C(CH$_3$)$_2$), 29.3 (CH(CH$_3$)$_2$), 29.2 (CH(CH$_3$)$_2$), 29.2 (C(CH$_3$)$_2$), 29.0 (CH(CH$_3$)$_2$), 28.4 (CH(CH$_3$)$_2$), 28.1 (CH(CH$_3$)$_2$), 27.7 (CH(CH$_3$)$_2$), 27.3 (CH(CH$_3$)$_2$), 27.2 (CH(CH$_3$)$_2$), 26.5 (CH(CH$_3$)$_2$), 26.2 (C(CH$_3$)$_2$), 26.0 (CH(CH$_3$)$_2$), 25.9 (CH(CH$_3$)$_2$), 24.3 (CH(CH$_3$)$_2$) ppm. ^{9}Be NMR (56 MHz, C_6D_6): $\delta = 20$ (fwmh ≈ 550 Hz) ppm. Elemental analysis (%) calc. for $C_{46}H_{68}BeN_2S$ [690.14 g mol^{-1}]: C 80.06, H 9.93, N 4.06, S 4.65; found.: C 79.70, H 10.09, N 3.94 S 4.17. UV-vis (benzene): $\lambda_{max} = 449$ nm.

Reduction of 1-S: To a solution of **1-S** (15.0 mg, 21.7 μmol) in 1 mL of Et_2O an excess of Li sand was added. The orange mixture turned brown within 5 min. Removal of all volatiles *in vacuo* provided a brown solid. An EPR spectrum and a few dark red crystals analyzed by X-ray crystallography confirmed the formation of **II** without other radical impurities. The identification of the sulfur-containing by-product via NMR spectroscopy was not possible due to the highly paramagnetic nature of the mixture.

Independent synthesis of (CAACH)SPh, 4-S: To a colorless solution of CAAC (30.0 mg, 105 μmol) in 0.5 mL benzene an excess of thiophenol was added. The removal of all volatiles *in vacuo* resulted in the isolation of **4-S** as a colorless solid (39.3 mg, 99.3 μmol, 93%). ^{1}H NMR (500.1 MHz, C_6D_6): $\delta = 7.24$ (m, 2H, CH_{Ar}), 7.00 (m, 3H, CH_{Ar}), 6.84 (m, 3H, CH_{Ar}), 4.97 (s, 1H, SC*H*), 3.97 (sept, $^3J = 6.7$ Hz, 1H, $CH(CH_3)_2$), 2.99 (sept, $^3J = 6.8$ Hz, 1H, $CH(CH_3)_2$), 1.93 ($^2J = 12.5$ Hz, 1H, CH_2), 1.78 ($^2J = 12.5$ Hz, 1H, CH_2), 1.61 (s, 3H, $C(CH_3)_2$), 1.59 (d, $^3J = 6.7$ Hz, 3H, $CH(CH_3)_2$), 1.43 (s, 3H, $C(CH_3)_2$), 1.32 (d, $^3J = 6.8$ Hz, 3H, $CH(CH_3)_2$), 1.18 (s, 3H, $C(CH_3)_2$), 1.16 (d, $^3J = 6.7$ Hz, 3H, $CH(CH_3)_2$), 0.93 (s, 3H, $C(CH_3)_2$), 0.76 (d, $^3J = 6.8$ Hz, 3H, $CH(CH_3)_2$) ppm. $^{13}C\{^1H\}$ NMR (125.8 MHz, C_6D_6): $\delta = 152.4$ (o-C_{Dip}), 150.1 (o-C_{Dip}), 138.9 (NC_{Dip}), 138.1 (SC_{Ar}), 134.7 (CH_{Ph}), 128.7 (CH_{Ph}), 127.6 (CH_{Ph}), 127.1(CH_{Dip}), 125.2 (CH_{Dip}), 125.0 (CH_{Dip}), 93.9 (SCHN), 62.7 3 ($C(CH_3)_2$), 57.2 (CH_2), 42.7 ($C(CH_3)_2$), 31.7 ($C(CH_3)_2$), 30.8 ($C(CH_3)_2$), 29.4 ($C(CH_3)_2$), 28.8 ($CH(CH_3)_2$), 28.7 ($C(CH_3)_2$), 28.4 ($CH(CH_3)_2$), 26.2 ($CH(CH_3)_2$), 25.7 ($CH(CH_3)_2$), 24.9 ($CH(CH_3)_2$), 24.6 ($CH(CH_3)_2$) ppm.

Synthesis of (CAAC)(CAACH)BeSePh, 1-Se: A solution of freshly prepared **II** (120 mg, 0.206 mmol, 1.00 equiv.) in 5 mL of Et_2O was cooled to −78 °C. Under exclusion of light Se_2Ph_2 (32.2 mg, 0.103 mmol, 0.50 equiv.) in Et_2O was added dropwise. The solution color changed instantly from brown to red and the solvent was removed *in vacuo*. The residual orange solid was washed with pentane until the washing phases became colorless, and then extracted with benzene. After removal of the solvent *in vacuo* **1-Se** was isolated as an orange solid (72.0 mg, 0.098 mmol, 47%). NMR data indicated contamination with small amounts of **4-Se**, by analogy with the data for **4-S** (attempts to synthesis **4-Se** independently by the addition of HSePh to CAAC failed, leading exclusively to the formation of $CAACH_2$ and Se_2Ph_2, which were identified by NMR-spectroscopic analysis). Elemental analysis data was obtained from a small amount of single crystals of **1-Se**. ^{1}H NMR (500.1 MHz, C_6D_6): $\delta = 8.04$ (m, 2H, o-CH_{Ph}), 7.36 (dd, $^3J = 7.6$ Hz, $^4J = 1.9$ Hz, 1H, m-CH_{Dip}), 7.23 (t, $^3J = 7.6$ Hz, 1H, p-CH_{Dip}), 7.08 (m, 6H, CH_{Ar}), 6.93 (dd, $^3J = 7.1$ Hz, $^4J = 2.2$ Hz, 1H, m-CH_{Dip}), 4.77 (sept, $^3J = 6.7$ Hz, 1H, $CH(CH_3)_2$), 3.58 (sept, $^3J = 6.7$ Hz, 1H, $CH(CH_3)_2$), 3.48 (br. sept, 1H, $CH(CH_3)_2$), 3.16 (s, 1H, Be*CH*), 2.41 (br. sept, 1H, $CH(CH_3)_2$), 1.99 (d, $^2J = 12.3$ Hz, 1H, CH_2), (d, $^2J = 12.3$ Hz, 1H, CH_2), 1.85 (br. d, $^3J = 5.9$ Hz, 3H, $CH(CH_3)_2$), 1.69 (br. d, $^3J = 5.9$ Hz, 3H, $CH(CH_3)_2$), 1.61 (s, 3H, $C(CH_3)_2$), 1.41 (d, $^3J = 6.8$ Hz, 3H, $CH(CH_3)_2$), 1.40 (d, $^3J = 6.8$ Hz, 3H, $CH(CH_3)_2$), 1.33-1.31 (two overlapping d and one s, 9H, 6H from $CH(CH_3)_2$ and 3H from $C(CH_3)_2$), 1.24 (d, $^2J = 12.9$ Hz, 1H, CH_2), 1.17 (s, 3H, $C(CH_3)_2$), 1.13 (m, 4H, 3H from $C(CH_3)_2$ and 1H from CH_2 detected by HSQC), 1.10 (s, 3H, CH_3, Me), 1.01 (s, 3H, $C(CH_3)_2$), 1.00 (d, $^3J = 6.8$ Hz, 3H, $CH(CH_3)_2$), 0.96 (d, $^3J = 6.7$ Hz, 3H, $CH(CH_3)_2$), 0.70 (br. s, 3H, $C(CH_3)_2$), 0.70 (br. s, 3H, $C(CH_3)_2$) ppm. $^{13}C\{^1H\}$ NMR (125.8 MHz, C_6D_6): $\delta = 254.4$ ($C_{carbene}$), 152.8 (o-C_{Ar}), 150.8 (o-C_{Ar}), 147.0 (NC_{Ar}), 145.7 (o-C_{Ar}), 145.4 (o-C_{Ar}), 136.6 (CH_{Ph}), 136.2 (CH_{Ph}), 135.7. (NC_{Ar}), 135.2 (SeC_{Ar}), 129.6 (CH_{Ph}), 128.34 (CH_{Ph}), 126.0 (CH_{Ph}), 125.0 (m-CH_{Dip}), 124.94 (p-CH_{Dip}), 124.5 (CH_{Ar}), 124.3 (CH_{Ar}), 124.2 (m-CH_{Ar}), 81.2 ($NC(CH_3)_2$), 72.6 (Be*C*HN), 63.7 ($NC(CH_3)_2$), 60.3 (CH_2), 55.8 ($C(CH_3)_2$), 51.0 (CH_2), 40.8 ($C(CH_3)_2$), 34.8 ($C(CH_3)_2$), 34.3 ($C(CH_3)_2$), 32.5 ($C(CH_3)_2$), 31.8 ($C(CH_3)_2$), 30.7 ($C(CH_3)_2$), 28.8 ($C(CH_3)_2$), 28.8 ($CH(CH_3)_2$), 28.7 ($C(CH_3)_2$), 28.6 ($CH(CH_3)_2$), 28.16 ($CH(CH_3)_2$), 27.7 ($CH(CH_3)_2$), 27.5 ($CH(CH_3)_2$), 27.2 ($CH(CH_3)_2$), 27.1 ($CH(CH_3)_2$), 27.0 ($CH(CH_3)_2$), 26.2 ($CH(CH_3)_2$), 25.8 ($CH(CH_3)_2$), 25.6 ($CH(CH_3)_2$), 25.1 ($C(CH_3)_2$), 23.8 ($CH(CH_3)_2$), ppm. ^{9}Be NMR (56 MHz, C_6D_6): $\delta = 22$ (fwmh ≈ 430 Hz) ppm. ^{77}Se NMR (95 MHz, C_6D_6): $\delta = 205$ ppm. Elemental analysis (%) calc. for $C_{46}H_{68}BeN_2Se$ [737.05 g mol^{-1}]: C 74.96, H 9.30, N 3.80; found.: C 74.09, H 9.27, N 3.56. UV-vis (benzene): $\lambda_{max} = 459$ nm.

Synthesis of (CAAC)(CAACH)BeTePh, 1-Te: A solution of freshly prepared **II** (240 mg, 0.413 mmol, 1.00 equiv.) in 5 mL of Et_2O was cooled to −78 °C. Under exclusion of light Te_2Ph_2 (84.5 mg, 0.207 mmol, 0.50 equiv.) in Et_2O was added dropwise. The solution color changed instantly from brown to red and the solvent was directly removed *in vacuo* in order to prevent decomposition. Crude **1-Te** was isolated as an orange solid (312 mg, 0.397 mmol, 75% purity). All attempts to recrystallize **1-Te** led to higher amounts of decomposition, therefore NMR data was collected on the crude product. Elemental analysis data was obtained from a small amount of single crystals of **1-Te**. ^{1}H NMR (500.1 MHz, C_6D_6): $\delta = 8.04$ (m, 2H, o-CH_{Ph}), 7.36 (dd, $^3J = 7.6$ Hz, $^4J = 1.8$ Hz, 1H, m-CH_{Dip}), 7.22 (t, $^3J = 7.6$ Hz, 1H, p-CH_{Dip}), 7.15 (m partly overlapping with solvent signal, 1H, CH_{Ar}) 7.09 (overlapping t and m, 2H, for t: $^3J = 7.6$ Hz, p-CH_{Dip}, for m: CH_{Ar}), 6.97 (m, 3H, CH_{Ar}), 6.90 (dd, $^3J = 7.6$ Hz, $^4J = 1.6$ Hz, 1H, m-CH_{Dip}), 5.08 (sept, $^3J = 6.7$ Hz, 1H, $CH(CH_3)_2$), 3.48 (sept, $^3J = 6.7$ Hz, 2H, $CH(CH_3)_2$), 3.22 (s, 1H, C*H*-CAAC), 2.34 (sept, $^3J = 6.3$ Hz 1H, $CH(CH_3)_2$), 2.05 (d, $^2J = 12.2$ Hz, 1H, CH_2), 1.96 (br. d, $^3J = 6.3$ Hz, 3H, $CH(CH_3)_2$), 1.89 (br. d, $^3J = 6.3$ Hz, 3H, $CH(CH_3)_2$), 1.77 (d, $^2J = 12.2$ Hz, 1H, CH_2), 1.61 (s, 3H, $C(CH_3)_2$), 1.55 (s, 3H, $C(CH_3)_2$), 1.44 (d, $^3J = 6.7$ Hz, 3H, $CH(CH_3)_2$), 1.39 (d, $^3J = 6.7$ Hz, 3H, $CH(CH_3)_2$), 1.31 (d, $^3J = 6.7$ Hz, 1H, $CH(CH_3)_2$), 1.25 (d, $^3J = 6.7$ Hz, 1H, $CH(CH_3)_2$), 1.19 (s, 3H, $C(CH_3)_2$), 1.16 (d, 1H, CH_2, detected by HSQC), 1.10 (s, 3H, $C(CH_3)_2$), 1.07 (d, ^{3}J = 6.7 Hz, 3H, $CH(CH_3)_2$), 0.96 (d, 1H, $^2J = 12.6$ Hz, CH_2), 0.94 (d, ^{3}J = 6.7 Hz, 3H, $CH(CH_3)_2$), 0.90 (s, 3H, $C(CH_3)_2$), 0.84 (s, 3H, $C(CH_3)_2$), 0.64 (s, 3H, $C(CH_3)_2$), 0.61 (s, 3H, $C(CH_3)_2$) ppm. $^{13}C\{^1H\}$ NMR (125.8 MHz, C_6D_6): $\delta = 254.6$ ($C_{carbene}$, detected by HMBC), 153.1 (o-C_{Dip}), 150.8 (o-C_{Dip}), 147.7 (NC_{Dip}), 146.2 (o-C_{Dip}), 145.3 (o-C_{Dip}), 145.3. (NC_{Dip}), 142.5 (o-CH_{Ph}), 138.6 (TeC_{Ph}), 136.2 (NC_{Dip}) 130.0 (CH_{Ph}), 128.3 (CH_{Ph}), 127.9 (CH_{Ph}, detected by HSQC), 126.5 (CH_{Dip}), 125.7 (CH_{Dip}), 125.5 (CH_{Dip}), 125.4 (p-CH_{Dip}), 124.9 (CH_{Dip}), 124.5 (m-CH_{Dip}), 81.5 ($NC(CH_3)_2$), 74.0 (BeCHN), 64.2 ($NC(CH_3)_2$), 60.9 (CH_2), 55.9 ($C(CH_3)_2$), 51.2 (CH_2), 41.1 ($C(CH_3)_2$), 36.8 ($C(CH_3)_2$), 34.7 ($C(CH_3)_2$), 33.5 ($C(CH_3)_2$), 32.8 ($C(CH_3)_2$), 31.1 ($C(CH_3)_2$), 30.6 ($C(CH_3)_2$), 29.1 ($CH(CH_3)_2$), 29.0 ($C(CH_3)_2$), 28.7 ($CH(CH_3)_2$), 28.4 ($CH(CH_3)_2$), 28.1 ($CH(CH_3)_2$), 28.1 ($CH(CH_3)_2$), 28.0 ($CH(CH_3)_2$), 27.8 ($CH(CH_3)_2$), 27.7 ($CH(CH_3)_2$), 26.5 ($CH(CH_3)_2$), 26.4 ($CH(CH_3)_2$), 26.1 ($CH(CH_3)_2$), 24.7 ($C(CH_3)_2$), 23.9 ($CH(CH_3)_2$) ppm. ^{9}Be NMR (56 MHz, C_6D_6): $\delta = 24$ (fwmh ≈ 420 Hz) ppm. ^{125}Te NMR (158 MHz, C_6D_6): $\delta = 157$ ppm. Elemental analysis (%) calc. for $C_{46}H_{68}BeN_2Te$ [785.68 g mol^{-1}]: C 70.32, H 8.72, N 3.57; found.: C 69.36, H 8.83, N 3.38. UV-vis (benzene): $\lambda_{max} = 417$ nm.

Synthesis of (CAAC)Be(SPh)(C_4Ph_4H), 5-S: Compound **III** (100 mg, 154 μmol, 1.00 equiv.) was dissolved in 10 mL of benzene and PhSH (16.9 mg, 154 μmol, 15.8 μL, 1.00 equiv.) was added with an Eppendorf pipette. Upon addition the solution changed instantly from bright yellow to colorless. Removal of all volatiles *in vacuo* provided a colorless solid, which was washed with pentane (3 × 2 mL) and recrystallized from a benzene/hexane mixture to yield **5-S** as colorless crystals (101 mg, 132.7 μmol, 86%). ^{1}H NMR (500.1 MHz, C_6D_6): $\delta = 7.73$ (br d, 3H, $^3J = 7.4$ Hz, $CH_{vinyl} + CH_{Ph}$), 7.39 (d, 2H, $^3J = 7.4$ Hz, CH_{Ph}), 7.28 (d, 2H, $^3J = 7.4$ Hz, CH_{Ph}), 7.24 (t, 1H, $^3J = 7.7$ Hz, p-CH_{Dip}), 7.15–7.14 (m, 2H, m-CH_{Dip}), 7.13–7.08 (m, 4H, CH_{Ph}), 7.04–6.99 (m, 2H, CH_{Ph}), 6.99–6.93 (m, 4H, CH_{Ph}), 6.83–6.77 (m, 4H, CH_{SPh}), 6.74 (br t, 2H, $^3J = 7.6$ Hz, m-CH_{Ph}), 6.64 (tt, 1H, $^3J = 7.4$ Hz, $^4J = 1.3$ Hz, p-CH_{SPh}), 6.18 (br s, 2H, CH_{Ph}), 3.20 (sept, 1H, $^3J = 6.5$ Hz, $CH(CH_3)_2$), 2.86 (sept, 1H, $^3J = 6.7$ Hz, $CH(CH_3)_2$), 1.70 (d, 3H, $^3J = 6.7$ Hz, $CH(CH_3)_2$), 1.58 (s, 3H, $C(CH_3)_2$), 1.43-1.36 (m, 7H, $CH_2 + C(CH_3)_2 + CH(CH_3)_2$), 1.33 (d, 1H, $^2J = 12.9$ Hz, CH_2), 1.17 (d, 3H, $^3J = 6.7$ Hz, $CH(CH_3)_2$), 1.11 (d, 3H, $^3J = 6.5$ Hz, $CH(CH_3)_2$), 0.97 (s, 3H, $C(CH_3)_2$), 0.77 (s, 3H, $C(CH_3)_2$) ppm. $^{13}C\{^1H\}$ NMR (125 MHz, C_6D_6): $\delta = 249.3$ ($C_{carbene}$), 150.7 (BeCCC), 150.4 (BeCCC), 149.3 (BeCCC), 146.3

(*o*-C_{Dip}), 145.8 (*o*-C_{Dip}), 143.5 (*i*-C_{Ph}), 142.1 (*i*-C_{Ph}), 141.2 (*i*-C_{Ph}), 138.5 (*i*-C_{Ph}), 134.9 (NC_{Dip}), 134.3 (*C*H$_{Ph}$), 131.7 (*C*H$_{Ph}$), 131.2 (*C*H$_{Ph}$), 130.6 (*C*H$_{Ph}$), 128.2 (*C*H$_{vinyl}$), 128.0 (*C*H$_{Ph}$), 127.9 (*C*H$_{Ph}$), 127.4 (*C*H$_{Ph}$), 127.1 (*C*H$_{Ph}$), 127.0 (*m*-*C*H$_{Dip}$), 126.8 (*C*H$_{Ph}$), 126.7 (*C*H$_{Ph}$), 125.7 (*p*-*C*H$_{Dip}$), 125.1 (*C*H$_{Ph}$), 124.0 (*C*H$_{Ph}$), 123.3 (*C*H$_{Ph}$), 82.0 (N*C*(CH$_3$)$_2$), 56.4 (*C*(CH$_3$)$_2$), 51.2 (*C*H$_2$), 30.8 (C(*C*H$_3$)$_2$), 30.5 (C(*C*H$_3$)$_2$), 29.6 (*C*H(CH$_3$)$_2$), 29.3 (*C*H(CH$_3$)$_2$), 29.1 (C(*C*H$_3$)$_2$), 28.2 (CH(*C*H$_3$)$_2$), 27.4 (CH(*C*H$_3$)$_2$), 27.2 (C(*C*H$_3$)$_2$), 25.5 (CH(*C*H$_3$)$_2$), 23.7 (CH(*C*H$_3$)$_2$), ppm. ^{9}Be NMR (56.24 MHz, C_6D_6): $\delta = 18.0$ (fwmh ≈ 580 Hz) ppm. Elemental analysis (%) calc. for $C_{54}H_{57}BeNS$ [761.13 g mol^{-1}]: C 85.21, H 7.55, N 1.18, S 4.21; found.: C 84.84, H 7.82, N 1.88, S 4.16.

(CAAC)Be(SePh)(C_4Ph_4H), 5-Se: Compound **III** (158.0 mg, 243 μmol, 1.00 equiv.) was dissolved in 10 mL of toluene and PhSeH (38.1 mg, 243 μmol, 25.8 μL, 1.00 equiv.) was added with an Eppendorf pipette. Upon addition the solution changed instantly from bright yellow to colorless. Removal of all volatiles *in vacuo* provided a colorless solid, which was washed with pentane (4×10 mL) to yield **5-Se** as a colorless solid (77.6 mg, 96.0 μmol, 40 %). ^{1}H NMR (500.1 MHz, C_6D_6): $\delta = 7.99$ (br s, 1H, C*H*$_{vinyl}$), 7.89 (d, 2H, $^3J = 7.3$ Hz, C*H*$_{Ph}$), 7.44 (br d, 2H, $^3J = 6.07$ Hz, C*H*$_{Ph}$), 7.31 (d, 2H, $^3J = 7.4$ Hz, *o*-CH$_{SePh}$), 7.22 (t, 1H, $^3J = 7.8$ Hz, *p*-C*H*$_{Dip}$), 7.15–7.12 (m, 2H, *m*-C*H*$_{Dip}$), 7.11–7.07 (m, 4H, C*H*$_{Ph}$), 7.03–7.00 (m, 2H, C*H*$_{Ph}$), 6.97 (t, 4H, ^3J = 8.3 Hz, C*H*$_{Ph}$), 6.83–6.76 (m, 4H, C*H*$_{Ph}$), 6.68 (br t, 2H, $^3J = 7.3$ Hz, C*H*$_{Ph}$), 6.64 (t, 1H, $^3J = 7.4$ Hz, *p*-C*H*$_{SePh}$), 6.07 (br s, 2H, C*H*$_{Ph}$), 3.18 (br s, 1H, C*H*(CH$_3$)$_2$), 2.84 (sept, 1H, $^3J = 6.7$ Hz, *CH*(CH$_3$)$_2$), 1.70 (br s, 3H, CH(C*H*$_3$)$_2$), 1.57 (s, 3H, CH(C*H*$_3$)$_2$), 1.40-1.39 (m, 7H, CH(C*H*$_3$)$_2$ + CH(C*H*$_3$)$_2$ + C*H*$_2$), 1.29 (d, 1H, $^2J = 12.9$ Hz, C*H*$_2$), 1.16 (d, 3H, ^3J = 6.7 Hz, CH(C*H*$_3$)$_2$), 1.11 (d, 2H, $^3J = 6.7$ Hz, CH(C*H*$_3$)$_2$), 0.95 (s, 3H, CH(C*H*$_3$)$_2$), 0.76 (s, 3H, CH(C*H*$_3$)$_2$) ppm. ^{13}C{^{1}H} NMR (125 MHz, C_6D_6): $\delta = 249.2$ (*C*$_{carbene}$), 150.4 (Be*C*CC), 148.7 (Be*C*CC), 146.1 (Be*C*CC), 145.8 (*o*-*C*$_{Dip}$), 143.5 (*i*-*C*$_{Ph}$), 141.4 (*i*-*C*$_{Ph}$), 138.5 (*i*-*C*$_{Ph}$), 136.5 (*C*H$_{Ph}$), 134.9 (N*C*$_{Dip}$), 134.0 (*i*-*C*$_{Ph}$), 131.6 (*C*H$_{Ph}$), 131.1 (*C*H$_{Ph}$), 131.0 (*C*H$_{Ph}$), 130.6 (*p*-*C*H$_{Dip}$), 130.2 (*C*H$_{Ph}$), 130.0 (*C*H$_{Ph}$), 128.4 (*C*H$_{vinyl}$), 127.3 (*C*H$_{Ph}$), 127.1 (*C*H$_{Ph}$), 127.1 (*C*H$_{Ph}$), 126.8 (*C*H$_{Ph}$), 126.8 (*C*H$_{Ph}$), 125.8 (*m*-*C*H$_{Dip}$), 125.1 (*C*H$_{Ph}$), 124.7 (*C*H$_{Ph}$), 123.2 (*C*H$_{Ph}$), 82.0 (N*C*(CH$_3$)$_2$), 56.0 (*C*(CH$_3$)$_2$), 51.2 (*C*H$_2$), 30.8 (C(*C*H$_3$)$_2$), 30.6 (C(*C*H$_3$)$_2$), 29.6 (*C*H(CH$_3$)$_2$), 29.3 (CH(*C*H$_3$)$_2$), 29.2 (CH(*C*H$_3$)$_2$), 28.6 (C(*C*H$_3$)$_2$), 27.5 (CH(*C*H$_3$)$_2$), 27.2 (C(*C*H$_3$)$_2$), 25.6 (CH(*C*H$_3$)$_2$), 23.7 (CH(*C*H$_3$)$_2$), ppm. ^{9}Be NMR (56.24 MHz, C_6D_6): $\delta = 20.6$ (fwmh ≈ 820 Hz) ppm. ^{77}Se NMR (95.38 MHz, C_6D_6): $\delta = 142.2$ ppm. Elemental analysis (%) calc. for $C_{54}H_{57}BeNSe$ [808.04 g mol^{-1}]: C 80.27, H 7.11, N 1.73; found.: C 79.59, H 7.29, N 1.67.

X-ray Crystallographic Details: The crystal data of **1-S** and **2-S** were collected on a Bruker X8-APEX II diffractometer with a CCD area detector and multi-layer mirror monochromated Mo$_{K\alpha}$ radiation. and the data of **1-Te** were collected on a XtaLAB Synergy, Dualflex, HyPix diffractometer with a Hybrid Pixel Array Detector and multi-layer mirror monochromated Cu$_{K\alpha}$ radiation. The crystal data of **1-Se**, **5-S** and **5-Se** were collected on a Rigaku XtaLAB Synergy-R diffractometer with a HPA area detector and multi-layer mirror monochromated Cu$_{K\alpha}$ radiation. The structures were solved using intrinsic phasing method,[51] refined with the ShelXL program[52] and expanded using Fourier techniques. All non-hydrogen atoms were refined anisotropically. Hydrogen atoms were included in structure factors calculations. All hydrogen atoms were assigned to idealized geometric positions, with the exception of those bound to boron, which were detected in the difference Fourier map and freely refined.

Crystallographic data: Deposition Number(s) 2239070 (**1-Se**), 2239071 (**5-Se**), 2239072 (**5-S**), 2239073 (**1-Te**), 2239074 (**1-S**) and 2239075 (**2-S**) contain(s) the supplementary crystallographic data for this paper. These data are provided free of charge by the joint Cambridge Crystallographic Data Centre and Fachinformationszentrum Karlsruhe Access Structures service.

Refinement details for 1-S: The asymmetric unit contains half of a highly disordered pentane molecule which has been treated as a diffuse contribution to the overall scattering without specific atom positions by Squeeze/Platon.[53] The number of electrons squeezed is 81 per unit cell, i. e. two molecules of pentane. **Crystal data for 1-S**: $C_{46}H_{68}BeN_2S$, $M_r = 690.09$, orange block, 0.90×0.598×0.544 mm, monoclinic space group $P2_1/n$, $a = 11.129(4)$ Å, $b = 19.7446(19)$ Å, $c = 20.705(4)$ Å, $\beta = 98.49(2)°$, $V = 4499.6(18)$ Å^3, $Z = 4$, $\rho_{calcd} = 1.019$ g·cm^{-3}, $\mu = 0.102$ mm^{-1}, $F(000) = 1512$, $T = 98(2)$ K, $R_1 = 0.0592$, $wR_2 = 0.1179$, 8862 independent reflections [$2\theta \leq 52.044°$] and 472 parameters.

Crystal data for 2-S: $C_{32}H_{41}BeNS_2$, $M_r = 512.79$, colorless block, 0.442×0.268×0.162 mm, monoclinic space group $P1_21/c1$, $a = 10.572(7)$ Å, $b = 16.531(10)$ Å, $c = 16.437(9)$ Å, $\beta = 93.26(3)°$, $V = 2868.(3)$ Å^3, $Z = 4$, $\rho_{calcd} = 1.188$ g cm^{-3}, $\mu = 0.207$ mm^{-1}, $F(000) = 1104$, $T = 100(2)$ K, $R_1 = 0.1013$, $wR_2 = 0.1555$, 6098 independent reflections [$2\theta \leq 53.54°$] and 333 parameters.

Refinement details for 1-Se: One outlying reflection affected by the beamstop was omitted (−10 5 10). **Crystal data for 1-Se**: $C_{46}H_{68}BeN_2Se$, $M_r = 736.99$, orange block, 0.099×0.054×0.051 mm, monoclinic space group $P2_1/n$, $a = 14.1507(3)$ Å, $b = 16.3373(3)$ Å, $c = 19.1014(4)$ Å, $\beta = 103.346(2)°$, $V = 4296.68(15)$ Å^3, $Z = 4$, $\rho_{calcd} = 1.139$ g cm^{-3}, $\mu = 1.400$ mm^{-1}, $F(000) = 1584$, $T = 99.99(13)$ K, $R_1 = 0.0617$, $wR_2 = 0.1103$, 8146 independent reflections [$2\theta \leq 140.15°$] and 467 parameters.

Crystal data for 1-Te: $C_{46}H_{68}BeN_2Te$, $M_r = 785.63$, orange block, 0.168×0.089×0.077 mm, monoclinic space group $P2_1/n$, $a = 14.23328(19)$ Å, $b = 18.78221(16)$ Å, $c = 17.0024(2)$ Å, $\beta = 108.9987(14)°$, $V = 4297.69(9)$ Å^3, $Z = 4$, $\rho_{calcd} = 1.214$ g cm^{-3}, $\mu = 5.681$ mm^{-1}, $F(000) = 1656$, $T = 99.9(6)$ K, $R_1 = 0.0577$, $wR_2 = 0.1392$, 8459 independent reflections [$2\theta \leq 144.254°$] and 467 parameters.

Crystal data for 5-S: $C_{54}H_{57}BeNS$, $M_r = 761.07$, colorless block, 0.165×0.152×0.095 mm, triclinic space group P1, $a = 11.4034(4)$ Å, $b = 12.2511(5)$ Å, $c = 16.1797(6)$ Å, $\alpha = 85.386(3)°$, $\beta = 82.815(3)°$, $\gamma = 82.948(3)°$, $V = 2220.79(15)$ Å^3, $Z = 2$, $\rho_{calcd} = 1.138$ g cm^{-3}, $\mu = 0.905$ mm^{-1}, $F(000) = 816$, $T = 99.99(10)$ K, $R_1 = 0.0807$, $wR_2 = 0.2388$, 8989 independent reflections [$2\theta \leq 151.122°$] and 522 parameters.

Refinement details for 5-Se: The asymmetric unit contains half a benzene molecule disordered on an inversion center, modelled as PART −1, and another benzene molecule with a twofold rotational disorder in a 64 : 36 ratio. Both molecules were idealized with AFIX 66 and their ADPs restrained with SIMU 0.01. **Crystal data for 5-Se**: $C_{63}H_{66}BeNSe$, $M_r = 925.13$, colourless plate, 0.315×0.229×0.076 mm, triclinic space group P1, $a = 12.1407(3)$ Å, $b = 12.4209(3)$ Å, $c = 18.1676(4)$ Å, $\alpha = 72.113(2)°$, $\beta = 83.680(2)°$, $\gamma = 80.230(2)°$, $V = 2564.50(11)$ Å^3, $Z = 2$, $\rho_{calcd} = 1.198$ g cm^{-3}, $\mu = 1.279$ mm^{-1}, $F(000) = 978$, $T = 99.97(10)$ K, $R_1 = 0.0561$, $wR_2 = 0.1462$, 10085 independent reflections [$2\theta \leq 149.948°$] and 649 parameters.

Computational details: All calculations were carried out using the Gaussian 16, Revision C.01,[54] the ADF 2019.304[55–56] and the ORCA 5.0[57] quantum chemistry program packages. Geometry optimizations for **1-S**, **1-Se** and **1-Te** were performed at the ωB97X-D[58]/Def2-SVP[59] level of theory. This level was chosen after a preliminary benchmark investigation using distinct DFT functionals (see Table S1 in the Supporting Information). All optimized geometries were characterized as minima on the corresponding potential energy surfaces by vibrational frequency calculations, which revealed that all eigenvalues of the Hessian matrices are positive. Plots of the frontier molecular orbitals (MOs) are shown in Figure S33 in the Supporting Information.

The vertical and adiabatic energy gaps between the closed-shell singlet and the triplet states were obtained at the DLPNO-

CCSD(T)[60–63] /Def2-TZVP[59] level of theory (see Table S2 in the Supporting Information). Given their large adiabatic singlet-triplet gaps of >35 kcal mol^{-1}, the **1-E** systems are accurately described by single reference methods and possess closed-shell singlet ground states.

To analyze the bonding situations in the different systems, Wiberg bond indices (WBIs)[64] and Mayer bond orders (MBOs)[65] of the Be–E bonds were calculated at the ωB97X–D/Def2-TZVP level of theory, using the Multiwfn[66] tool. These values are shown in Table S3 in the Supporting Information, which also highlights that experimental and calculated Be–E bond lengths show excellent agreement.

Further bonding investigation of **1-S**, **1-Se** and **1-Te** was performed by the energy decomposition analysis with the natural orbital for chemical valence (EDA-NOCV)[67–69] method at the PBE0-D3[70,71] /TZ2P[72] level of theory (see main text for further details). The main results of the different bonding situations considered are displayed in Table S4 in the Supporting Information.

Gibbs free energies for the reactions of **II** with E_2Ph_2 to yield **1-E** (Scheme S1, E = S, Se, Te) were calculated at the ωB97X–D/Def2-TZVP/SMD(toluene)[73] level of theory, while ωB97X–D/Def2-SVP was used for the zero-point corrections (see Table S5 in the Supporting Information).

Supporting Information contains NMR and UV-vis spectra for new compounds, as well as further solid-state structures and computational details.

Acknowledgements

This project was funded by the Julius-Maximilians-Universität Würzburg and Deutsche Forschungsgemeinschaft (DFG, German Research Foundation) – project numbers 466754611 and BR1149/25-1. L.M. thanks the Verband der Chemischen Industrie (VCI) for a Kekulé fellowship. Open Access funding enabled and organized by Projekt DEAL.

Conflict of Interests

The authors declare no conflict of interest.

Data Availability Statement

The data that support the findings of this study are available from the corresponding author upon reasonable request.

Keywords: beryllium chalcogenide · crystallographic analysis · EDA-NOCV · radical reactions

[1] M. G. MacMurdo, P. M. Mroz, D. A. Culver, R. Dweik, L. Maier, *Chest* **2020**, *158*, 2458–2466.
[2] K. Kreiss, G. A. Day, C. R. Schuler, *Annu. Rev. Public Health* **2007**, *28*, **259–277**.
[3] D. M. Hollins, M. A. McKinley, C. Williams, A. Wiman, D. Fillos, P. S. Chapman, A. K. Madl, *Crit. Rev. Toxicol.* **2009**, *39*, 1–32.
[4] K. M. Fromm, *Coord. Chem. Rev.* **2020**, *408*, 213193.
[5] P. M. Chapple, Y. Sarazin, *Eur. J. Inorg. Chem.* **2020**, 3321–3346.
[6] B. M. Wolf, R. Anwander, *Chem. Eur. J.* **2019**, *25*, 8190–8202.
[7] D. Mukherjee, D. Schuhknecht, J. Okuda, *Angew. Chem. Int. Ed.* **2018**, *57*, 9590–9602.
[8] M. Westerhausen, A. Koch, H. Görls, S. Krieck, *Chem. Eur. J.* **2017**, *23*, 1456–1483.
[9] M. S. Hill, D. J. Liptrot, C. Weetman, *Chem. Soc. Rev.* **2016**, *45*, 972–988.
[10] M. M. Montero-Campillo, O. Mó, M. Yáñez, I. Alkorta, J. Elguero, *Adv. Inorg. Chem.* **2019**, *73*, 73–121.
[11] B. Rösch, S. Harder, *Chem. Commun.* **2021**, *57*, 9354–9365.
[12] J. K. Buchanan, P. G. Plieger, *Chem. Lett.* **2021**, *50*, 227–234.
[13] M. R. Buchner, *Chem. Commun.* **2020**, *56*, 8895–8907.
[14] M. R. Buchner, *Chem. Eur. J.* **2019**, *25*, 12018–12036.
[15] L. C. Perera, O. Raymond, W. Henderson, P. J. Brothers, P. G. Plieger, *Coord. Chem. Rev.* **2017**, *352*, 264–290.
[16] K. J. Iversen, S. A. Couchman, D. J. D. Wilson, J. L. Dutton, *Coord. Chem. Rev.* **2015**, *297*, 40–48.
[17] M. Arrowsmith, H. Braunschweig, M. A. Celik, T. Dellermann, R. D. Dewhurst, W. C. Ewing, K. Hammond, T. Kramer, I. Krummenacher, J. Mies, K. Radacki, J. K. Schuster, *Nat. Chem.* **2016**, *8*, 890–894.
[18] G. Wang, J. E. Walley, D. A. Dickie, S. Pan, G. Frenking, R. J. Gilliard Jr. *J. Am. Chem. Soc.* **2020**, *142*, 4560–4564.
[19] C. Czernetzki, M. Arrowsmith, F. Fantuzzi, A. Gärtner, T. Tröster, I. Krummenacher, F. Schorr, H. Braunschweig, *Angew. Chem. Int. Ed.* **2021**, *60*, 20776–20780.
[20] M. Gimferrer, S. Danes, E. Vos, C. B. Yildiz, I. Corral, A. Jana, P. Salvador, D. M. Andrada, *Chem. Sci.* **2022**, *13*, 6583–6591.
[21] S. Pan, G. Frenking, *Chem. Sci.* **2023**, *14*, 379–383.
[22] M. Gimferrer, S. Danes, E. Vos, C. B. Yildiz, I. Corral, A. Jana, P. Salvador, D. M. Andrada, *Chem. Sci.* **2023**, *14*, 384–392.
[23] D. K. Roy, T. Tröster, F. Fantuzzi, R. D. Dewhurst, C. Lenczyk, K. Radacki, C. Pranckevicius, B. Engels, H. Braunschweig, *Angew. Chem. Int. Ed.* **2021**, *60*, 3812–3819.
[24] K. Li, L. Qian, X. Li, Y. Ma, W. Zhou, *Front. Energy Res.* **2021**, *9*, Article 669832.
[25] T. Sandu, W. P. Kirk, *Phys. Rev. B* **2006**, *73*, Article 235307.
[26] O. Maksimov, *Rev. Adv. Mater. Sci.* **2005**, *9*, 178–183.
[27] S. Chadwick, U. Englich, K. Ruhlandt-Senge, *Angew. Chem. Int. Ed.* **1998**, *37*, 3007–3009.
[28] R. Han, G. Parkin, *Inorg. Chem.* **1993**, *32*, 4968–4982.
[29] G. E. Coates, B. R. Francis, *J. Chem. Soc. A* **1971**, 160–164.
[30] G. E. Coates, A. H. Fishwick, *J. Chem. Soc. A* **1968**, 635–640.
[31] N. A. Bell, *J. Chem. Soc. A* **1966**, 542–544.
[32] H. Funk, R. Masthof, *J. Prakt. Chem.* **1963**, *22*, 250–254.
[33] M. Niemeyer, P. P. Power, *Inorg. Chem.* **1997**, *36*, 4688–4696.
[34] K. Ruhlandt-Senge, R. A. Bartlett, M. M. Olmstead, P. P. Power, *Inorg. Chem.* **1993**, *32*, 1724–1728.
[35] R. Andersen, N. A. Bell, G. E. Coates, *J. Chem. Soc. Dalton Trans.* **1972**, 577–582.
[36] H. Nöth, D. Schlosser, *Chem. Ber.* **1988**, *121*, 1711–1713.
[37] While the test reactions between CAAC, Se_2Ph_2 or Te_2Ph_2 generate **3-Se** or **3-Te**, respectively, as the major product, that with S_2Ph_2 does not generate **3-S**.
[38] Given that the analogous oxygen-based reagent, O_2Ph_2, is not available, **II** was reacted with the TEMPO (2,2,6,6-tetramethylpiperidinyloxyl) radical. Independent of the reaction conditions, however, the reaction was very unselective and no molecular CAAC-stabilized beryllium alkoxide could be isolated.
[39] B. Cordero, V. Gómez, A. E. Platero-Prats, M. Revés, J. Echeverría, E. Cremades, F. Barragán, S. Alvarez, *Dalton Trans.* **2008**, 2832–2838.
[40] J.-D. Chai, M. Head-Gordon, *Phys. Chem. Chem. Phys.* **2008**, *10*, 6615–6620.
[41] F. Weigend, R. Ahlrichs, *Phys. Chem. Chem. Phys.* **2005**, *7*, 3297–3305.
[42] K. B. Wiberg, *Tetrahedron* **1968**, *24*, 1083–1096.
[43] I. Mayer, *Chem. Phys. Lett.* **1983**, *97*, 270–274.
[44] G. te Velde, F. M. Bickelhaupt, E. J. Baerends, C. Fonseca Guerra, S. J. A. van Gisbergen, J. G. Snijders, T. Ziegler, *J. Comput. Chem.* **2001**, *22*, 931–967.
[45] M. Ernzerhof, G. E. Scuseria, *J. Chem. Phys.* **1999**, *110*, 5029–5036.
[46] C. Adamo, V. Barone, *J. Chem. Phys.* **1999**, *110*, 6158–6170.
[47] S. Grimme, J. Antony, S. Ehrlich, H. Krieg, *J. Chem. Phys.* **2010**, *132*, Article 154104.
[48] L. Zhao, S. Pan, G. Frenking, *J. Chem. Phys.* **2022**, *157*, Article 034105.
[49] L. Zhao, M. Hermann, W. H. E. Schwarz, G. Frenking, *Nature Rev. Chem.* **2019**, *3*, 48–63.

[50] V. Lavallo, Y. Canac, C. Präsang, B. Donnadieu, G. Bertrand, *Angew. Chem. Int. Ed. Engl.* **2005**, *44*, 5705–5709.
[51] G. Sheldrick, *Acta Crystallogr.* **2015**, *A71*, 3–8.
[52] G. Sheldrick, *Acta Crystallogr.* **2008**, *A64*, 112–122.
[53] A. L. Spek, *Acta Crystallogr.* **2015**, *C71*, 9–18.
[54] Gaussian 16 (Revision C.01), M. J. Frisch, G. W. Trucks, H. B. Schlegel, G. E. Scuseria, M. A. Robb, J. R. Cheeseman, G. Scalmani, V. Barone, G. A. Petersson, H. Nakatsuji, X. Li, M. Caricato, A. V. Marenich, J. Bloino, B. G. Janesko, R. Gomperts, B. Mennucci, H. P. Hratchian, J. V. Ortiz, A. F. Izmaylov, J. L. Sonnenberg, D. Williams-Young, F. Ding, F. Lipparini, F. Egidi, J. Goings, B. Peng, A. Petrone, T. Henderson, D. Ranasinghe, V. G. Zakrzewski, J. Gao, N. Rega, G. Zheng, W. Liang, M. Hada, M. Ehara, K. Toyota, R. Fukuda, J. Hasegawa, M. Ishida, T. Nakajima, Y. Honda, O. Kitao, H. Nakai, T. Vreven, K. Throssell, J. A. Montgomery, Jr., J. E. Peralta, F. Ogliaro, M. J. Bearpark, J. J. Heyd, E. N. Brothers, K. N. Kudin, V. N. Staroverov, T. A. Keith, R. Kobayashi, J. Normand, K. Raghavachari, A. P. Rendell, J. C. Burant, S. S. Iyengar, J. Tomasi, M. Cossi, J. M. Millam, M. Klene, C. Adamo, R. Cammi, J. W. Ochterski, R. L. Martin, K. Morokuma, O. Farkas, J. B. Foresman, D. J. Fox, Gaussian Inc., Wallingford CT, **2016**.
[55] G. te Velde, F. M. Bickelhaupt, E. J. Baerends, C. Fonseca Guerra, S. J. A. van Gisbergen, J. G. Snijders, T. Ziegler, *J. Comput. Chem.* **2001**, *22*, 821–967.
[56] ADF 2019.304, E. J. Baerends, T. Ziegler, A. J. Atkins, J. Autschbach, O. Baseggio, D. Bashford, A. Bérces, F. M. Bickelhaupt, C. Bo, P. M. Boerrigter, C. Cappelli, L. Cavallo, C. Daul, D. P. Chong, D. V. Chulhai, L. Deng, R. M. Dickson, J. M. Dieterich, F. Egidi, D. E. Ellis, M. van Faassen, L. Fan, T. H. Fischer, A. Förster, C. Fonseca Guerra, M. Franchini, A. Ghysels, A. Giammona, S. J. A. van Gisbergen, A. Goez, A. W. Götz, J. A. Groeneveld, O. V. Gritsenko, M. Grüning, S. Gusarov, F. E. Harris, P. van den Hoek, Z. Hu, C. R. Jacob, H. Jacobsen, L. Jensen, L. Joubert, J. W. Kaminski, G. van Kessel, C. König, F. Kootstra, A. Kovalenko, M. V. Krykunov, P. Lafiosca, E. van Lenthe, D. A. McCormack, M. Medves, A. Michalak, M. Mitoraj, S. M. Morton, J. Neugebauer, V. P. Nicu, L. Noodleman, V. P. Osinga, S. Patchkovskii, M. Pavanello, C. A. Peeples, P. H. T. Philipsen, D. Post, C. C. Pye, H. Ramanantoanina, P. Ramos, W. Ravenek, M. Reimann, J. I. Rodríguez, P. Ros, R. Rüger, P. R. T. Schipper, D. Schlüns, H. van Schoot, G. Schreckenbach, J. S. Seldenthuis, M. Seth, J. G. Snijders, M. Solà, M. Stener, M. Swart, D. Swerhone, V. Tognetti, G. te Velde, P. Vernooijs, L. Versluis, L. Visscher, O. Visser, F. Wang, T. A. Wesolowski, E. M. van Wezenbeek, G. Wiesenekker, S. K. Wolff, T. K. Woo, A. L. Yakovlev, SCM, Theoretical Chemistry, Vrije Universiteit, Amsterdam, The Netherlands, http://www.scm.com.
[57] F. Neese, F. Wennmohs, U. Becker, C. Riplinger, *J. Chem. Phys.* **2020**, *152*, 224108.
[58] J.-D. Chai, M. Head-Gordon, *Phys. Chem. Chem. Phys.* **2008**, *10*, 6615–6620.
[59] F. Weigend, R. Ahlrichs, *Phys. Chem. Chem. Phys.* **2005**, *7*, 3297–3305.
[60] Y. Guo, K. Sivalingam, E. F. Valeev, F. Neese, *J. Chem. Phys.* **2016**, *144*, 094111.
[61] C. Angeli, R. Cimiraglia, J.-P. Malrieu, *Chem. Phys. Lett.* **2001**, *350*, 297–305.
[62] C. Angeli, R. Cimiraglia, S. Evangelisti, T. Leininger, J.-P. Malrieu, *J. Chem. Phys.* **2001**, *114*, 10252–10264.
[63] C. Angeli, R. Cimiraglia, J.-P. Malrieu, *J. Chem. Phys.* **2002**, *117*, 9138–9153.
[64] K. B. Wiberg, *Tetrahedron* **1968**, *24*, 1083–1096.
[65] I. Mayer, *J. Comput. Chem.* **2007**, *28*, 204–221.
[66] T. Lu, *J. Comput. Chem.* **2012**, *33*, 580–592.
[67] T. Ziegler, A. Rauk, *Inorg. Chem.* **1979**, *18*, 1558–1565.
[68] T. Ziegler, A. Rauk, *Inorg. Chem.* **1979**, *18*, 1755–1759.
[69] M. Mitoraj, A. Michalak, T. Ziegler, *J. Chem. Theory Comput.* **2009**, *5*, 962–975.
[70] C. Adamo, V. Barone, *J. Chem. Phys.* **1999**, *110*, 6158–6170.
[71] S. Grimme, J. Antony, S. Ehrlich, H. Krieg, *J. Chem. Phys.* **2010**, *132*, 1541004.
[72] E. van Lenthe, E. J. Baerends, *J. Comput. Chem.* **2003**, *24*, 1142–1156.
[73] A. V. Marenich, C. J. Cramer, D. G. Truhlar, *J. Phys. Chem. B* **2009**, *113*, 6378–6396.

Manuscript received: May 4, 2023
Accepted manuscript online: May 22, 2023
Version of record online: ■■, ■■

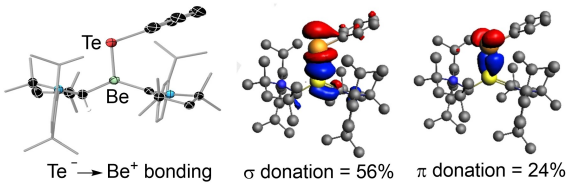

*C. Czernetzki, Dr. T. Tröster, L. Endres, F. Endres, Dr. M. Arrowsmith, Dr. A. Gärtner, Dr. F. Fantuzzi, Prof. Dr. H. Braunschweig**

1 – 9

Synthesis, Structural Characterization, and Bonding of Molecular Heavier Beryllium Chalcogenides

The reactions of a beryllium(I) radical with E_2Ph_2 (E = S, Se, Te) and of a beryllole with HEPh (E = S, Se) yield the corresponding beryllium phenylchalcogenides, including the first structurally authenticated beryllium selenide and telluride complexes. Calculations show that their Be–E bonds are best described as ionic, with Coulombic forces accounting for 56% of the attraction and orbital interactions dominated by the σ component.